Published in final edited form as:
Exp Neurol. 2012 March ; 234(1): 62–69. doi:10.1016/j.expneurol.2011.12.015.

Protection From Diabetes-Induced Peripheral Sensory Neuropathy –A Role For Elevated Glyoxalase I?

M.M. Jack, **J.M. Ryals**, and **D.E. Wright**
Department of Anatomy and Cell Biology, University of Kansas Medical Center, Kansas City, KS 66160

Abstract

Diabetic neuropathy is a common complication of diabetes mellitus with over half of all patients developing neuropathy symptoms due to sensory nerve damage. Diabetes-induced hyperglycemia leads to the accelerated production of advanced glycation end products (AGEs) that alter proteins, thereby leading to neuronal dysfunction. The glyoxalase enzyme system, specifically glyoxalase I (GLO1), is responsible for detoxifying precursors of AGEs, such as methylglyoxal and other reactive dicarbonyls. The purpose of our studies was to determine if expression differences of GLO1 may play a role in the development of diabetic sensory neuropathy. BALB/cJ mice naturally express low levels of GLO1, while BALB/cByJ express approximately 10-fold higher levels on a similar genetic background due to increased copy numbers of GLO1. Five weeks following STZ injection, diabetic BALB/cJ mice developed a 68% increase in mechanical thresholds, characteristic of insensate neuropathy or loss of mechanical sensitivity. This behavior change correlated with a 38% reduction in intraepidermal nerve fiber density (IENFD). Diabetic BALB/cJ mice also had reduced expression of mitochondrial oxidative phosphorylation proteins in Complex I and V by 83% and 47%, respectively. Conversely, diabetic BALB/cByJ mice did not develop signs of neuropathy, changes in IENFD, or alterations in mitochondrial protein expression. Reduced expression of GLO1 paired with diabetes-induced hyperglycemia may lead to neuronal mitochondrial damage and symptoms of diabetic neuropathy. Therefore, AGEs, the glyoxalase system, and mitochondrial dysfunction may play a role in the development and modulation of diabetic peripheral neuropathy.

Keywords

mice; diabetes; neuropathy; skin innervation; epidermis; glyoxalase I; dorsal root ganglion; peripheral nerve; mechanical sensitivity

Introduction

Diabetic neuropathy (DN) is secondary consequence of longstanding diabetes mellitus. Sensory neurons appear particularly vulnerable to elevated glucose and damage in diabetes mellitus (Zochodne, et al., 2008). Consequently, 50–70% of patients develop DN signs and symptoms throughout the course of the disease (Centers for Disease Control and Prevention,

For Correspondence: Douglas Wright, Department of Anatomy and Cell Biology, University of Kansas Medical Center, Kansas City, KS 66160, Phone: 913-588-2713, Fax: 913-588-2710, dwright@kumc.edu.

2011). Moreover, DN remains a growing problem in the United States and throughout the world with only limited symptomatic treatments (Edwards, et al., 2008).

Though the pathogenesis of DN is likely multifactorial, one mechanism leading to sensory neuron damage and dysfunction is the accumulation of a heterogeneous group of reactive sugars known as advanced glycation endproducts (AGEs) (Ahmed, 2005, Brownlee, 2005). AGEs can form via a number of pathways inside and outside the neuron. In particular, reactive dicarbonyls, a potent producer of AGEs, are formed as a normal by-product of glycolysis, lipid peroxidation, and degradation of glycated proteins (Ahmed and Thornalley, 2007, Thornalley, 2008). Each of these processes is enhanced in diabetes mellitus leading to an increased formation of toxic reactive dicarbonyls. Once formed, reactive dicarbonyls react with proteins, lipids, or nucleic acids forming AGEs and cause neuronal dysfunction (Thornalley, 2008).

The glyoxalase system functions to detoxify reactive dicarbonyls before they react with cellular components and form AGEs (Rabbani and Thornalley, 2011). The glyoxalase system is composed of two enzymes, glyoxalase I (GLO1) and glyoxalase II, that detoxify reactive dicarbonyls by converting them to lactic acid, thereby preventing the formation of AGEs (Thornalley, 2003). We have recently shown that in the peripheral nervous system, GLO1 is selectively expressed in small, unmyelinated peptidergic neurons and axons that comprise a subset of DRG neurons that are responsible for pain transmission (Jack, et al., 2011). While GLO1 has been investigated in other diabetic complications, its role in DN has remained largely uninvestigated.

GLO1 exists as a copy number variant (CNV) in many inbred strains mice (Williams, et al., 2009). In particular, BALB/cJ mice have a single copy, whereas a closely related substrain, BALB/cByJ mice, has multiple copies (Williams, et al., 2009). BALB/cJ and BALB/cByJ mice originated from the same parental strain and were separated in the 1930s (Bailey, 1978). Despite 80 years of segregated inbreeding, these two strains remain isogenic at all typed SNPs but have 11 genetic sites that have copy number variations (Velez, et al., 2010, Williams, et al., 2009). In particular, BALB/cJ have lost multiple copies of the region encompassing GLO1 (Williams, et al., 2009). Thus, BALB/cByJ and BALB/cJ mice express variable levels of GLO1 on similar genetic backgrounds.

Given the clear evidence showing GLO1 has a role in protecting against hyperglycemia-induced diabetic complications including nephropathy and endothelial dysfunction, GLO1 may also have a role in protecting sensory neurons from the damaging effects of diabetes mellitus (Ahmed, et al., 2008, Wautier and Schmidt, 2004). In this study, we took advantage of the natural genetic variation in substrains of BALB/c mice to investigate sensory damage in DN in strains expressing different amounts of GLO1. Our results BALB/cByJ mice appear to be protected against early neuropathy-related behavioral changes and sensory neuron damage, and this protection may be related to elevated GLO1.

Methods

Animals

Male BALB/cJ and BALB/cByJ mice (Jackson, Bar Harbor, ME) were purchased at 7 weeks, one week prior to the onset of experimental testing. BALB/cJ mice were housed one mouse per cage, while BALB/cByJ mice were housed two per cage in 12/12-h light/dark cycle under pathogen free conditions. Mice were given free access to standard rodent chow (Harlan Teklad 8,604, 4% kcal derived from fat) and water. All animal use was in accordance with NIH guidelines and conformed to principles specified by the University of Kansas Medical Center Animal Care and Use Protocol.

Diabetes Induction

Diabetes was induced in 8-week-old male BALB/cJ and BALB/cByJ mice. BALB/cJ and BALB/cByJ mice were injected with a single intraperitoneal injection of streptozocin (STZ) (260 mg/kg and 200 mg/kg body weight, respectively; Sigma, St. Louis, MO) dissolved in 10 mmol/L sodium citrate buffer, pH 4.5. Controls received sodium citrate buffer alone. Animals of either strain that did not develop hyperglycemia three days after the initial injection were re-injected with STZ (200 mg/kg body weight). Food was removed from all cages for 3 h before and after STZ injection. Animals did not receive insulin at any point in the study.

Glucose Measurements

Animal weights and blood glucose levels (glucose diagnostic reagents, Sigma, St. Louis, MO) were measured three days and one week after STZ injection. Both were then measured every week thereafter from tail vein sampling and decapitation blood pool for terminal measurements. Mice were considered diabetic if their fasting blood glucose level is greater than 200 mg/dl at every measurement.

Behavior Testing

Mice underwent training sessions on the four days prior to behavioral testing. Mice were placed into individual clear plastic cages on a wire mesh screen elevated 55 cm above the table. Mice were allowed to acclimate in their cages to the behavior room for 30 minutes and on the mesh grid for 15–45 minutes on the table during the training sessions, depending on the training day. Before each behavioral testing session, mice were allowed to acclimate to the behavior room in their cages for 30 minutes and to the wire mesh grid for 15 minutes. The up-down method was used to test mechanical sensitivity (Dixon, 1980). Briefly, a set of standard von Frey monofilaments (0.02, 0.07, 0.16, 0.4, 1.0, 2.0, 6.0, and 10.0 g) were used to assess mechanical sensitivity. Beginning with the 0.4 g monofilament, mice received a single application to the right hindpaw. Depending on the response of the mouse to the previous application, the next smaller filament was used if there was negative response or the next larger gram filament was used if there was a positive response. This was repeated on each mouse until there was a change from either a positive response to negative response or vice versa. Four trials after the change were then conducted with 5 min intervals between applications. A positive response was considered a brisk withdrawal of the paw to which the force was applied. Five negative responses were recorded as the maximum threshold or 10 g, while 5 positive responses were recorded as the minimum threshold or 0.02 g. The 50% threshold was calculated for each mouse and group means were determined as previous described (Chaplan, et al., 1994). Baseline behavior was measured before diabetes induction. Afterwards, all animals were tested weekly for 6 weeks.

Tissue Preparation

DRG were rapidly isolated and excised, immediately frozen in liquid nitrogen, and stored at −80°C. DRG were sonicated for 5 intervals of 10 sec each in 50 μL Cell Extraction Buffer (Invitrogen, Carlsbad, CA) with protease inhibitor cocktail (Sigma, St. Louis, MO), 200 mM NaF, and 200 mM Na_3VO_4. The homogenates were incubated on ice for 30 mins before centrifugation at 7000 rpm for 10 mins at 4°C. Protein concentrations were determined using the Bio-Rad protein assay based on the Bradford assay (Bio-Rad, Sydney, NSW, Australia).

Glyoxalase I Expression

Samples containing 100 μg of protein from total DRG homogenates were separated by electrophoresis through 4–20% SDS-PAGE gels (125 V, 1.5 h, 4°C) and transferred onto nitrocellulose paper (35 mA, overnight, 4°C). Nitrocellulose membranes were blocked with

blocking buffer (3% non-fat milk and 0.05% Tween-20 in phosphate buffered saline) for 1 hour at room temperature to block non-specific binding sites. This was followed by overnight incubation with a goat anti-GLO1 primary antibody (R&D Systems, Minneapolis, MN) diluted 1:5000 in blocking buffer at 4°C. The donkey anti-goat IgG-HRP (Santa Cruz, Santa Cruz, CA) secondary antibody was used diluted 1:2500 in blocking buffer at RT for 1 hour.

Nitrocellulose membranes were stripped using Restore Plus Western Blot Stripping Buffer (Pierce, Rockford, IL). This was followed by 1-hour incubation with actin primary antibody (Millipore, Billerica, MA) diluted 1:100,000 in blocking buffer at RT. The donkey anti-mouse IgG-HRP secondary antibody (Santa Cruz, Santa Cruz, CA) was used diluted 1:2500 in blocking buffer at RT for 1 hour. The chemiluminescent signal was acquired using Supersignal West Femto Maximum Sensitivity Substrate (Pierce, Rockford, IL) and a CCD camera (BioSpectrum Imaging System, UVP, Upland, CA). Labworks Analysis Software (UVP, Upland, CA) was used to quantify densitometry readings.

Nerve Conduction Velocity

Nerve conduction velocity was conducted as previously described on a Viasys Healthcare TECA Synergy (Muller, et al., 2008, Stevens, et al., 2000). Animals were deeply anesthetized with Avertin (1.25% v/v tribromoethanol, 2.5% tert-amyl alcohol, dH_2O; 200 mg/kg body weight). Corneal reflexes were checked and body temperature was monitored and maintained at 37°C throughout the procedure. Motor nerve conduction velocities (MNCVs) were obtained by measuring compound muscle action potentials using supramaximal stimulation (9.9 mA) at the ankle distally and at the sciatic notch proximally. The average of three independent recordings was obtained from the first interosseous muscle. Sensory nerve conduction velocity (SNCV) was measured behind the medial malleolus with a 0.5-ms square wave pulse using the smallest current to elicit a response (2.4 mA), stimulating at the digital nerve of the second toe. SNCV was the average of 10 recordings.

Intraepidermal Nerve Fiber Density

Cutaneous innervation of the footpad was assessed in nondiabetic and diabetic mice after six weeks of diabetes. The right footpad skin was harvested from mice at the time of sacrifice and immersion fixed in Zamboni's fixative (4% paraformaldehyde, 14% saturated picric acid, 0.1 M phosphate buffered saline; pH 7.4) for 1 hour on ice. Footpads were washed in PBS twice and placed in PBS overnight at 4°C. Footpads were then cryoprotected in 30% sucrose overnight at 4°C. 30 μm serial sections were cut and placed on Superfrost Plus microscope slides (Fischer, Chicago, IL). Immunohistochemistry was performed as previous described (Christianson, et al., 2007, Johnson, et al., 2008). Briefly, tissue sections were blocked in Primary Incubation Solution containing SuperBlock buffer (Pierce, Rockford, IL) with 1.5% normal donkey serum, 0.5% porcine gelatin, and 0.5% Triton X-100 for 1 hour at RT. Sections were then incubated in the primary antibody solution containing 1:1 Primary Incubation Solution and SuperBlock buffer with rabbit anti-PGP9.5 primary antibody (1:400) overnight at 4°C. A donkey anti-rabbit secondary antibody (Alexa 555, 1:2000, Molecular Probes, Eugene, OR) in 1X PBST was incubated for 1 hour at 4°C. Small cutaneous, PGP9.5+ fibers that crossed the dermal-epidermal junction were quantified in three areas from three tissue sections from each footpad. The length of the dermal-epidermal junction was measured and intraepidermal nerve fiber density (IENFD) was expressed as the number of fibers per millimeter.

Mitochondrial Enzyme Expression

15 μg of protein from total DRG homogenates was separated by electrophoresis (150 V, 2 h, 4°C) on a 10–20% Tris-Glycine SDS-PAGE gels (Invitrogen, Carlsbad, CA) and transferred onto nitrocellulose paper (150 mA, 2 h, 4°C). Membranes were blocked in 5% non-fat milk and 0.05% Tween-20 in phosphate buffered saline either overnight at 4°C or 3 hours at RT. An antibody cocktail against mitochondrial electron transport proteins (MS601, MitoSciences, Eugene, OR) was diluted 205X in 1% milk and incubated at RT for 2 h. The donkey anti-mouse IgG-HRP (Santa Cruz, Santa Cruz, CA) secondary antibody was used diluted 1:2000 in blocking buffer at RT for 2 hours. The chemiluminescence signal was acquired using Supersignal West Femto Maximum Sensitivity Substrate (Pierce, Rockford, IL) and a CCD camera (BioSpectrum Imaging System, UVP, Upland, CA). LabWorks Analysis Software (UVP, Upland, CA) was used to quantify densitometry readings. All bands were normalized for actin expression.

Statistics

Data are expressed as mean ± SEM. *n* is the number of animals per given experimental setting. Differences were analyzed using ANOVA followed by Bonferroni's test, as appropriate. Significance was defined as $p \leq 0.05$.

Results

Blood Glucose and Weights

More than 90% of mice of both strains injected with STZ developed diabetes shortly after injection. As early as 1 week following STZ injection, diabetic mice displayed markedly increased blood glucose levels. At the earliest time point, diabetic BALB/cByJ mice had an average blood glucose of 325.495 ± 15.943 mg/dl and diabetic BALB/cJ mice had an average blood glucose of 341.206 ± 19.735 mg/dl (Figure 1a). The elevated blood glucose persisted and worsened throughout the study with diabetic BALB/cByJ mice having an average blood glucose of 510.871 ± 19.737 mg/dl and diabetic BALB/cJ mice having an average blood glucose of 535.698 ± 12.120 mg/dl after 6 weeks of diabetes (Figure 1a). At all time points measured, diabetic mice from both strains had similar blood glucose levels that were not statistically different (Figure 1a).

Diabetic mice displayed other characteristic symptoms of hyperglycemia including polyuria, polydipsia, and limited weight gain. Throughout the study, nondiabetic BALB/cByJ mice gained on average 6.9 ± 0.3 g and, similarly, nondiabetic BALB/cJ mice gained 5.6 ± 0.6 g (Figure 1b). Conversely, diabetic mice had reduced weight gain, as is characteristic of diabetic mouse models. Diabetic BALB/cByJ gained 2.1 ± 0.5 g from baseline, while diabetic BALB/cJ gained 0.2 ± 0.9 g (Figure 1b). Throughout the study, the average weight of diabetic mice was not significantly different between the two strains.

Behavioral Measures

The responses of mice to von Frey monofilaments were used to determine mechanical sensitivity of the right hindpaw by measuring the 50% gram threshold weekly. No difference existed in baseline behavioral measures between strains with thresholds of 2.429 ± 0.425 g for BALB/cByJ and 2.076 ± 0.323 g for BALB/cJ ($p = 0.5110$) (Figure 2). The baseline thresholds were similar for all four groups tested with nondiabetic BALB/cByJ mice, diabetic BALB/cByJ, nondiabetic BALB/cJ, and diabetic BALB/cJ having baseline thresholds of 2.152 ± 0.428 g, 3.119 ± 0.781 g, 2.975 ± 0.549 g, and 1.389 ± 0.329 g, respectively.

After five weeks of severe hyperglycemia, diabetic BALB/cJ mice develop increased mechanical thresholds that are indicative of insensate neuropathy (Figure 2). The 50% withdrawal threshold of diabetic BALB/cJ mice at five weeks after STZ injection was 5.899 ± 0.977 g, while nondiabetic BALB/cByJ and BALB/cJ mice had thresholds of 2.805 ± 0.581g and 1.888 ± 0.373 g, respectively. Decreased mechanical sensitivity was also present after six weeks of diabetes in diabetic BALB/cJ mice reaching nearly a 77% increase from baseline. Diabetic BALB/cJ mice at had mechanical thresholds of 6.138 ± 0.945 g, while nondiabetic BALB/cByJ and BALB/cJ mice had thresholds of 2.362 ± 0.415 g and 2.022 ± 0.344 g, respectively. This behavioral change is similar in time course and severity to that seen in STZ-treated C57BL/6 mice (Christianson, et al., 2007, Johnson, et al., 2008).

Despite having significant hyperglycemia for six weeks, diabetic BALB/cByJ mice do not develop thresholds significantly different from baseline (Figure 2). Mechanical thresholds of diabetic BALB/cByJ mice are also not significantly different from nondiabetic BALB/cByJ or BALB/cJ at any time point. On the other hand, diabetic BALB/cByJ mice had significantly lower thresholds compared to diabetic BALB/cJ mice at both five and six weeks post-STZ (2.739 ± 0.299 g vs. 5.899 ± 0.977g and 2.555 ± 0.408 g vs. 6.138 ± 0.945 g).

GLO1 Expression in Diabetes

After six weeks of diabetes, Western blot was used to determine GLO1 expression differences between strains and the impact of diabetes on GLO1 levels. Nondiabetic BALB/cByJ mice had significantly higher expression of GLO1 in the DRG compared to nondiabetic BALB/cJ (1.000 ± 0.084 vs. 0.132 ± 0.097) (Figure 3). Since GLO1 expression remained unchanged from nondiabetic levels following diabetes induction in both diabetic BALB/cJ and BALB/cByJ, diabetic BALB/cJ mice had significantly lower expression than diabetic BALB/cByJ mice (0.091 ± 0.001 vs. 0.852 ± 0.134) (Figure 3). Combined, BALB/cByJ mice had 8–15-fold higher GLO1 expression compared to BALB/cJ mice.

Intraepidermal Nerve Fiber Density Following Diabetes Induction

After six weeks of diabetes, the pan-neuronal marker, PGP-9.5 was used to quantify cutaneous C-fibers in the hindpaw epidermis. IENFD was similar between strains of nondiabetic mice (Figure 4a, b, and e). Control BALB/cByJ mice had 80.3 ± 5.3 fibers/mm in the right hindpaw which was no different from control BALB/cJ mice that had 89.3 ± 4.5 fibers/mm. Conversely, diabetic BALB/cJ mice had 38% and 31% loss of cutaneous innervation compared to nondiabetic BALB/cJ and BALB/cByJ, respectively (Figure 4a, b, d, and e). On the other hand, diabetic BALB/cByJ mice, which did not display mechanical deficits, showed IENFD similar to both nondiabetic strains (Figure 4a, b, c, and e). Thus, diabetic BALB/cJ mice also showed a 35% reduction of IENFD compared to diabetic BALB/cByJ mice.

Nerve Conduction Velocity

Both motor (MNCV) and sensory nerve conduction velocities (SNCV) were measured at the end of the six-week study in all four groups. SNCV was not significantly different between any groups (p=0.055) (Figure 5a). While nondiabetic BALB/cByJ and BALB/cJ mice had similar MNCV (50.825 ± 1.380 m/s vs. 55.120 ± 1.088 m/s, respectively), recordings identified motor dysfunction in both diabetic strains (Figure 5b). Diabetic BALB/cByJ mice had MNCVs of 42.456 ± 1.716 m/s, which was significantly lower compared to both nondiabetic BALB/cByJ and BALB/cJ strains. However, diabetic BALB/cJ mice only had significant slowing of MNCV when compared to nondiabetic BALB/cJ mice. The MNCV of diabetic BALB/cJ mice was similar to diabetic BALB/cByJ mice (Figure 5b).

Mitochondrial Dysfunction

The expression of mitochondrial oxidative phosphorylation proteins was measured in the DRG to determine potential mechanisms leading to neuronal dysfunction. No strain differences were apparent in the levels of Complex I subunit NDUFB8, Complex II FeS subunit, Complex III subunit Core 2, or Complex V subunit alpha between nondiabetic BALB/cByJ and BALB/cJ mice (Figure 6a, b, c, and d). Strikingly, Complex I expression was dramatically reduced in diabetic BALB/cJ compared to the other three groups (Figure 6d). The expression of the NDUFB8 subunit was 83%, 81%, and 81% lower compared to nondiabetic BALB/cJ, nondiabetic BALB/cByJ, and diabetic BALB/cByJ, respectively (Figure 6d). While Complex II and III expression was not significantly different between groups (Figure 6b and c), Complex V was also reduced by 47% and 51% in diabetic BALB/cJ mice compared to nondiabetic BALB/cJ and diabetic BALB/cByJ mice (Figure 6a).

Discussion

In this study, two genetically similar strains of inbred mice that are natural genetic variants of GLO1 were used to investigate the potential role of GLO1 in development and modulation of diabetic neuropathy. We have previously shown GLO1 is predominately expressed in small, unmyelinated peptidergic neurons in the DRG, suggesting this DRG sensory neurons may be more or less vulnerable to hyperglycemia-damage depending on the level of GLO1 expression. Here, our results reveal that BALB/cByJ mice have increased expression of GLO1 and are protected from the development of neuropathy symptoms following six weeks of hyperglycemia, while BALB/cJ mice develop increased mechanical thresholds and hypoalgesia characteristic of insensate neuropathy. Other parameters of neuron dysfunction are present in both diabetic strains including slowing of MNCV, however, only diabetic BALB/cJ mice display reduced C-fiber innervation of the hindpaw. It is plausible to suggest that these anatomical and behavior changes are a consequence of differential levels of reactive dicarbonyl-derived AGEs that modify mitochondrial oxidative phosphorylation structural proteins and may lead to mitochondrial dysfunction (Brouwers, et al., 2010, Brownlee, 2005). Collectively, these results suggest that reduced expression of GLO1 may prevent efficient breakdown of reactive-dicarbonyl that cause mitochondrial damage, loss of peripheral C-fiber innervation, and the development of mechanical insensitivity in diabetic neuropathy.

Numerous studies have shown overexpression of GLO1 to be protective against reactive dicarbonyl damage (Brouwers, et al., 2010, Brouwers, et al., 2010, Gangadhariah, et al., 2010, Morcos, et al., 2008, Schlotterer, et al., 2009). However, few studies have investigated the importance of GLO1 at physiological levels. To our knowledge, this is the first to investigate variable expression in peripheral nerves and its potential role in the development of diabetic neuropathy. A week after the onset of reduced mechanical sensitivity, GLO1 expression in the DRG of diabetic BALB/cJ mice remains similar to that of nondiabetic mice. Although expression and activity in diabetes are likely species-, strain-, and tissue-dependent, our studies suggest that GLO1 expression is not altered by diabetes in the DRG of these two strains of inbred mice. However, due to the known CNV, GLO1 expression in both nondiabetic and diabetic BALB/cJ mice is significantly lower than either nondiabetic or diabetic BALB/cByJ mice. Higher expression of GLO1 may limit carbonyl stress and ultimately reduce AGE-mediated damage, at least early in the disease process.

The loss of cutaneous nerve fibers, nerve conduction velocity, and behavioral measures have all been used to assess the presence of sensory nerve damage characteristic of diabetic neuropathy in both rodents and human patients. Diabetic BALB/cJ mice develop loss of epidermal innervation, reduced nerve conduction velocities, and increased mechanical thresholds, as do majority of diabetic patients. At least early in the disease course, diabetic

BALB/cByJ mice are protected from developing signs of DN that diabetic BALB/cJ mice develop. Similarly, a sizable percentage of patients, nearly 30–40%, do not develop classic overt neuropathy signs and symptoms even after years of diabetes mellitus. Recently, a study of Joslin Gold Medalists, patients who have survived type I diabetes mellitus for over 50 years, determined that glycemic control was unrelated to the development of diabetic complications (Sun, et al., 2011). However, those patients with higher concentrations of AGEs, including methylglyoxal-derived *N*-(carboxyethyl)lysine, were 2.5 times more likely to suffer from neuropathy (Sun, et al., 2011). Those authors and others have suggested that certain patients may have an abundance of protective mechanisms that allow them to remain complication free.

This suggests that underlying genetic differences in certain diabetic patients can protect against damage from methylglyoxal. Since GLO1 is the major detoxification system of reactive dicarbonyls, it is plausible that differences in production and activity of the enzyme influences AGE production and the development and/or modulation of DN. Studies have recognized various SNPs, null alleles, and CNVs of GLO1 in humans (Gale, et al., 2004, Gale and Grant, 2004, Redon, et al., 2006, Sparkes, et al., 1983). While a number of studies have measured increased AGEs in diabetic patients in the skin and peripheral nerve (Meerwaldt, et al., 2005, Misur, et al., 2004, Sugimoto, et al., 1997, Yu, et al., 2006), limited investigation into the variability of protective mechanisms, particularly in these tissues, has occurred and may help explain why some patients develop DN and others do not.

Investigation into early signs and symptoms of neuronal dysfunction is critical to understanding the mechanisms driving the pathogenesis of diabetic neuropathy. A week after the onset of reduced mechanical sensitivity in diabetic BALB/cJ mice, the expression of structural components of mitochondrial oxidative phosphorylation proteins Complex I and V is dramatically reduced. Evidence linking reactive dicarbonyls with mitochondrial dysfunction has been mounting (Rabbani and Thornalley, 2008). In a *C. elegan* model of aging, the reactive dicarbonyl-derived AGE, MGH1, modified mitochondrial proteins leading to increased ROS which was attenuated with GLO1 overexpression (Morcos, et al., 2008). *In vitro* investigation utilizing a neuroblastoma cell line found ATP and mitochondrial membrane potential were both reduced following exposure to methylglyoxal (de Arriba, et al., 2007). Further evidence suggesting increased GLO1 expression protects against mitochondrial damage was recently published utilizing a transgenic rat model overexpressing GLO1. Diabetic transgenic rats showed increased GLO1 expression, reduced levels of plasma reactive dicarbonyls and AGEs, and higher expression of mitochondrial oxidative phosphorylation proteins compared to wild type diabetic rats (Brouwers, et al., 2010).

Mitochondrial dysfunction has also been implicated in the pathogenesis of diabetic neuropathy. Similar to our data, Chowdhury *et al.* observed reduced expression of NDUFS3, one component of the iron-sulfur protein of Complex I, in STZ-diabetic rats (Chowdhury, et al., 2010). They have also observed alterations in other mitochondrial proteins, including components of oxidative phosphorylation including ATP synthase (Akude, et al., 2011). Functionally, rates of respiration and activity of oxidative phosphorylation complexes are reduced in in the peripheral nervous system of diabetic rats that result from proteome alterations (Chowdhury, et al., 2010). With evidence linking oxidative phosphorylation proteins modified by reactive dicarbonyls with mitochondrial dysfunction, diabetic BALB/cByJ mice could be protected from these proteome alterations due to increased GLO1 production. Thus, genetic differences in protective mechanisms, particularly of GLO1, could play a role in preventing early mitochondrial dysfunction that may underlie sensory neuron damage and DN symptoms.

Acknowledgments

This work was supported by the Juvenile Diabetes Research Foundation and NIH RO1NS43314 to D.E. Wright, and by the Kansas IDDRC, P30 NICHD HD 002528.

References

1. Ahmed N. Advanced glycation endproducts--role in pathology of diabetic complications. Diabetes Res Clin Pract. 2005; 67:3–21. [PubMed: 15620429]
2. Ahmed N, Thornalley PJ. Advanced glycation endproducts: what is their relevance to diabetic complications? Diabetes Obes Metab. 2007; 9:233–245. [PubMed: 17391149]
3. Ahmed U, Dobler D, Larkin SJ, Rabbani N, Thornalley PJ. Reversal of hyperglycemia-induced angiogenesis deficit of human endothelial cells by overexpression of glyoxalase 1 in vitro. Ann N Y Acad Sci. 2008; 1126:262–264. [PubMed: 18448827]
4. Akude E, Zherebitskaya E, Chowdhury SK, Smith DR, Dobrowsky RT, Fernyhough P. Diminished superoxide generation is associated with respiratory chain dysfunction and changes in the mitochondrial proteome of sensory neurons from diabetic rats. Diabetes. 2011; 60:288–297. [PubMed: 20876714]
5. Bailey, DW. Sources of subline divergence and their relative importance for sublines of six major inbred strains of mice. In: HCM, editor. Origins of inbred mice. Academic Press; New York: 1978. p. 197-213.
6. Brouwers O, Niessen PM, Ferreira I, Miyata T, Scheffer PG, Teerlink T, Schrauwen P, Brownlee M, Stehouwer CD, Schalkwijk CG. Overexpression of glyoxalase-I reduces hyperglycemia-induced levels of advanced glycation endproducts and oxidative stress in diabetic rats. J Biol Chem. 2010
7. Brouwers O, Niessen PM, Haenen G, Miyata T, Brownlee M, Stehouwer CD, De Mey JG, Schalkwijk CG. Hyperglycaemia-induced impairment of endothelium-dependent vasorelaxation in rat mesenteric arteries is mediated by intracellular methylglyoxal levels in a pathway dependent on oxidative stress. Diabetologia. 2010; 53:989–1000. [PubMed: 20186387]
8. Brownlee M. The pathobiology of diabetic complications: a unifying mechanism. Diabetes. 2005; 54:1615–1625. [PubMed: 15919781]
9. Centers for Disease Control and Prevention. National diabetes fact sheet: national estimates and general information on diabetes and prediabetes in the United States. U.S. Department of Health and Human Services, Centers for Disease Control and Prevention; Atlanta, GA: 2011.
10. Chaplan SR, Bach FW, Pogrel JW, Chung JM, Yaksh TL. Quantitative assessment of tactile allodynia in the rat paw. J Neurosci Methods. 1994; 53:55–63. [PubMed: 7990513]
11. Chowdhury SK, Zherebitskaya E, Smith DR, Akude E, Chattopadhyay S, Jolivalt CG, Calcutt NA, Fernyhough P. Mitochondrial respiratory chain dysfunction in dorsal root ganglia of streptozotocin-induced diabetic rats and its correction by insulin treatment. Diabetes. 2010; 59:1082–1091. [PubMed: 20103706]
12. Christianson JA, Ryals JM, Johnson MS, Dobrowsky RT, Wright DE. Neurotrophic modulation of myelinated cutaneous innervation and mechanical sensory loss in diabetic mice. Neuroscience. 2007; 145:303–313. [PubMed: 17223273]
13. de Arriba SG, Stuchbury G, Yarin J, Burnell J, Loske C, Munch G. Methylglyoxal impairs glucose metabolism and leads to energy depletion in neuronal cells--protection by carbonyl scavengers. Neurobiol Aging. 2007; 28:1044–1050. [PubMed: 16781798]
14. Dixon WJ. Efficient analysis of experimental observations. Annu Rev Pharmacol Toxicol. 1980; 20:441–462. [PubMed: 7387124]
15. Edwards JL, Vincent AM, Cheng HT, Feldman EL. Diabetic neuropathy: mechanisms to management. Pharmacol Ther. 2008; 120:1–34. [PubMed: 18616962]
16. Gale CP, Futers TS, Summers LK. Common polymorphisms in the glyoxalase-1 gene and their association with pro-thrombotic factors. Diab Vasc Dis Res. 2004; 1:34–39. [PubMed: 16305054]
17. Gale CP, Grant PJ. The characterisation and functional analysis of the human glyoxalase-1 gene using methods of bioinformatics. Gene. 2004; 340:251–260. [PubMed: 15475166]

18. Gangadhariah MH, Mailankot M, Reneker L, Nagaraj RH. Inhibition of methylglyoxal-mediated protein modification in glyoxalase I overexpressing mouse lenses. J Ophthalmol. 2010; 2010:274317. [PubMed: 20671953]
19. Jack MM, Ryals JM, Wright DE. Characterisation of glyoxalase I in a streptozocin-induced mouse model of diabetes with painful and insensate neuropathy. Diabetologia. 2011
20. Johnson MS, Ryals JM, Wright DE. Early loss of peptidergic intraepidermal nerve fibers in an STZ-induced mouse model of insensate diabetic neuropathy. Pain. 2008; 140:35–47. [PubMed: 18762382]
21. Meerwaldt R, Links TP, Graaff R, Hoogenberg K, Lefrandt JD, Baynes JW, Gans RO, Smit AJ. Increased accumulation of skin advanced glycation end-products precedes and correlates with clinical manifestation of diabetic neuropathy. Diabetologia. 2005; 48:1637–1644. [PubMed: 16021416]
22. Misur I, Zarkovic K, Barada A, Batelja L, Milicevic Z, Turk Z. Advanced glycation endproducts in peripheral nerve in type 2 diabetes with neuropathy. Acta Diabetol. 2004; 41:158–166. [PubMed: 15660198]
23. Morcos M, Du X, Pfisterer F, Hutter H, Sayed AA, Thornalley P, Ahmed N, Baynes J, Thorpe S, Kukudov G, Schlotterer A, Bozorgmehr F, El Baki RA, Stern D, Moehrlen F, Ibrahim Y, Oikonomou D, Hamann A, Becker C, Zeier M, Schwenger V, Miftari N, Humpert P, Hammes HP, Buechler M, Bierhaus A, Brownlee M, Nawroth PP. Glyoxalase-1 prevents mitochondrial protein modification and enhances lifespan in Caenorhabditis elegans. Aging Cell. 2008; 7:260–269. [PubMed: 18221415]
24. Muller KA, Ryals JM, Feldman EL, Wright DE. Abnormal muscle spindle innervation and large-fiber neuropathy in diabetic mice. Diabetes. 2008; 57:1693–1701. [PubMed: 18362211]
25. Rabbani N, Thornalley PJ. Dicarbonyls linked to damage in the powerhouse: glycation of mitochondrial proteins and oxidative stress. Biochem Soc Trans. 2008; 36:1045–1050. [PubMed: 18793186]
26. Rabbani N, Thornalley PJ. Glyoxalase in diabetes, obesity and related disorders. Semin Cell Dev Biol. 2011
27. Redon R, Ishikawa S, Fitch KR, Feuk L, Perry GH, Andrews TD, Fiegler H, Shapero MH, Carson AR, Chen W, Cho EK, Dallaire S, Freeman JL, Gonzalez JR, Gratacos M, Huang J, Kalaitzopoulos D, Komura D, MacDonald JR, Marshall CR, Mei R, Montgomery L, Nishimura K, Okamura K, Shen F, Somerville MJ, Tchinda J, Valsesia A, Woodwark C, Yang F, Zhang J, Zerjal T, Armengol L, Conrad DF, Estivill X, Tyler-Smith C, Carter NP, Aburatani H, Lee C, Jones KW, Scherer SW, Hurles ME. Global variation in copy number in the human genome. Nature. 2006; 444:444–454. [PubMed: 17122850]
28. Schlotterer A, Kukudov G, Bozorgmehr F, Hutter H, Du X, Oikonomou D, Ibrahim Y, Pfisterer F, Rabbani N, Thornalley P, Sayed A, Fleming T, Humpert P, Schwenger V, Zeier M, Hamann A, Stern D, Brownlee M, Bierhaus A, Nawroth P, Morcos M. C. elegans as model for the study of high glucose-mediated life span reduction. Diabetes. 2009; 58:2450–2456. [PubMed: 19675139]
29. Sparkes RS, Sparkes MC, Crist M, Anderson CE. Glyoxalase I “null” allele in a new family: identification by abnormal segregation pattern and quantitative assay. Hum Genet. 1983; 64:146–147. [PubMed: 6885048]
30. Stevens MJ, Obrosova I, Cao X, Van Huysen C, Greene DA. Effects of DL-alpha-lipoic acid on peripheral nerve conduction, blood flow, energy metabolism, and oxidative stress in experimental diabetic neuropathy. Diabetes. 2000; 49:1006–1015. [PubMed: 10866054]
31. Sugimoto K, Nishizawa Y, Horiuchi S, Yagihashi S. Localization in human diabetic peripheral nerve of N(epsilon)-carboxymethyllysine-protein adducts, an advanced glycation endproduct. Diabetologia. 1997; 40:1380–1387. [PubMed: 9447944]
32. Sun JK, Keenan HA, Cavallerano JD, Asztalos BF, Schaefer EJ, Sell DR, Strauch CM, Monnier VM, Doria A, Aiello LP, King GL. Protection from retinopathy and other complications in patients with type 1 diabetes of extreme duration: the joslin 50-year medalist study. Diabetes Care. 2011; 34:968–974. [PubMed: 21447665]
33. Thornalley PJ. Glyoxalase I--structure, function and a critical role in the enzymatic defence against glycation. Biochem Soc Trans. 2003; 31:1343–1348. [PubMed: 14641060]

34. Thornalley PJ. Protein and nucleotide damage by glyoxal and methylglyoxal in physiological systems--role in ageing and disease. Drug Metabol Drug Interact. 2008; 23:125–150. [PubMed: 18533367]

35. Velez L, Sokoloff G, Miczek KA, Palmer AA, Dulawa SC. Differences in aggressive behavior and DNA copy number variants between BALB/cJ and BALB/cByJ substrains. Behav Genet. 2010; 40:201–210. [PubMed: 20033273]

36. Wautier JL, Schmidt AM. Protein glycation: a firm link to endothelial cell dysfunction. Circ Res. 2004; 95:233–238. [PubMed: 15297385]

37. Williams, Rt; Lim, JE.; Harr, B.; Wing, C.; Walters, R.; Distler, MG.; Teschke, M.; Wu, C.; Wiltshire, T.; Su, AI.; Sokoloff, G.; Tarantino, LM.; Borevitz, JO.; Palmer, AA. A common and unstable copy number variant is associated with differences in Glo1 expression and anxiety-like behavior. PLoS One. 2009; 4:e4649. [PubMed: 19266052]

38. Yu Y, Thorpe SR, Jenkins AJ, Shaw JN, Sochaski MA, McGee D, Aston CE, Orchard TJ, Silvers N, Peng YG, McKnight JA, Baynes JW, Lyons TJ. Advanced glycation end-products and methionine sulphoxide in skin collagen of patients with type 1 diabetes. Diabetologia. 2006; 49:2488–2498. [PubMed: 16955213]

39. Zochodne DW, Ramji N, Toth C. Neuronal targeting in diabetes mellitus: a story of sensory neurons and motor neurons. Neuroscientist. 2008; 14:311–318. [PubMed: 18660461]

Highlights

- Glyoxalase I protects against damaging effects of advanced glycation end products.
- We examine two strains of mice that naturally express different levels of GLO1. u
- Diabetic BALB/cJ mice with low levels develop several classic signs of neuropathy.
- Diabetic BALB/cByJ mice with high levels do not develop signs of neuropathy.
- These mice provide a new tool to explore the role of GLO1 and AGE-related damage.

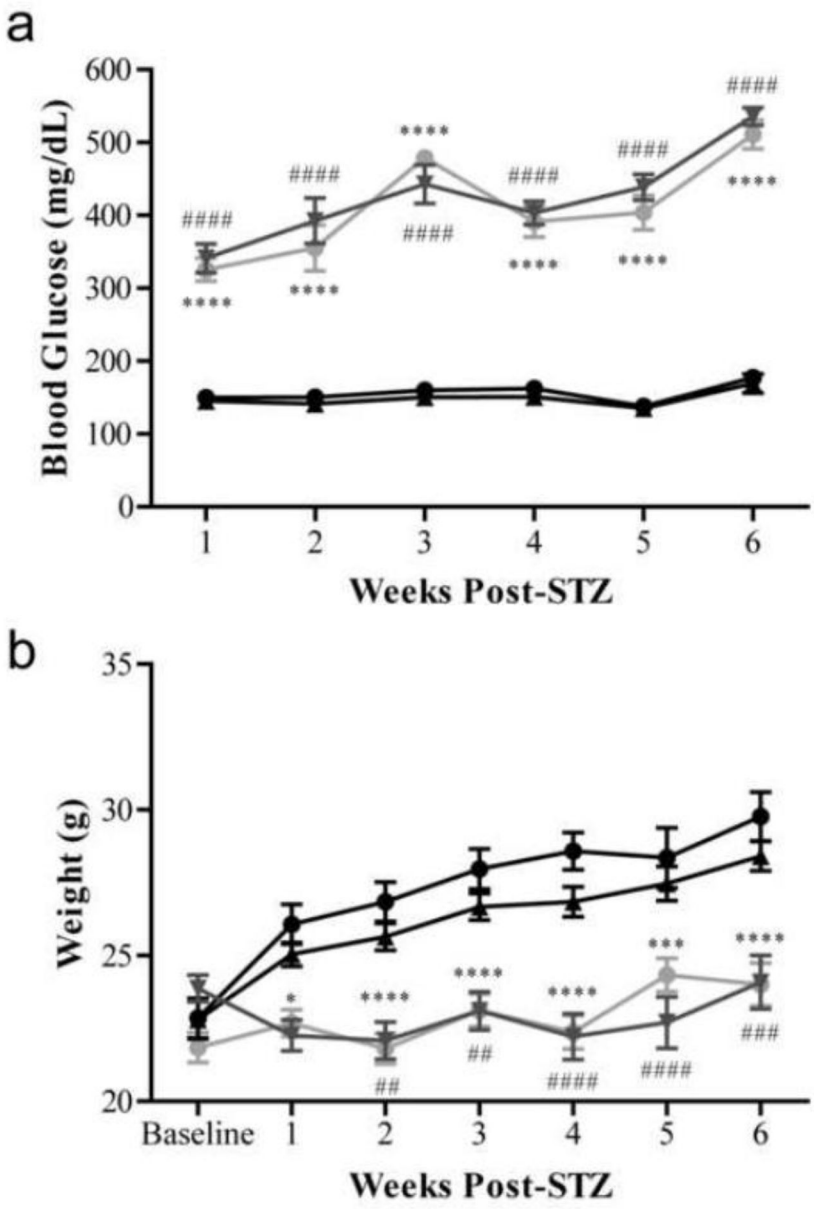

Figure 1. Diabetic BALB/cByJ and BALB/cJ mice display characteristic features of diabetes including hyperglycemia and smaller body weight

Blood glucose (a) and weights (b) of nondiabetic and diabetic BALB/cByJ and BALB/cJ measured weekly for six weeks. (a) Diabetic BALB/cByJ (gray circles, $n = 15$) and BALB/cJ (gray triangles, $n = 15$) showed similar blood glucose measures each week, which was significantly different than nondiabetic BALB/cByJ (black circles, $n = 10$) and BALB/cJ (black triangles, $n = 10$) ($p < 0.0001$). (b) Diabetic BALB/cByJ (gray circles, $n = 15$) and diabetic BALB/cJ (gray triangles, $n = 15$) had reduced weight gain compared to nondiabetic mice (black circles, BALB/cByJ, $n = 10$ and black triangles, BALB/cJ, $n = 10$) ($p < 0.0001$). Data are presented as means ± SEM. *$p < 0.05$ vs. nondiabetic BALB/cByJ mice. ***$p < 0.001$ vs. nondiabetic BALB/cByJ mice. ****$p < 0.0001$ vs. nondiabetic BALB/cByJ mice. ##$p < 0.01$ vs. nondiabetic BALB/cJ mice. ###$p < 0.001$ vs. nondiabetic BALB/cJ mice. ####$p < 0.0001$ vs. nondiabetic BALB/cJ mice.

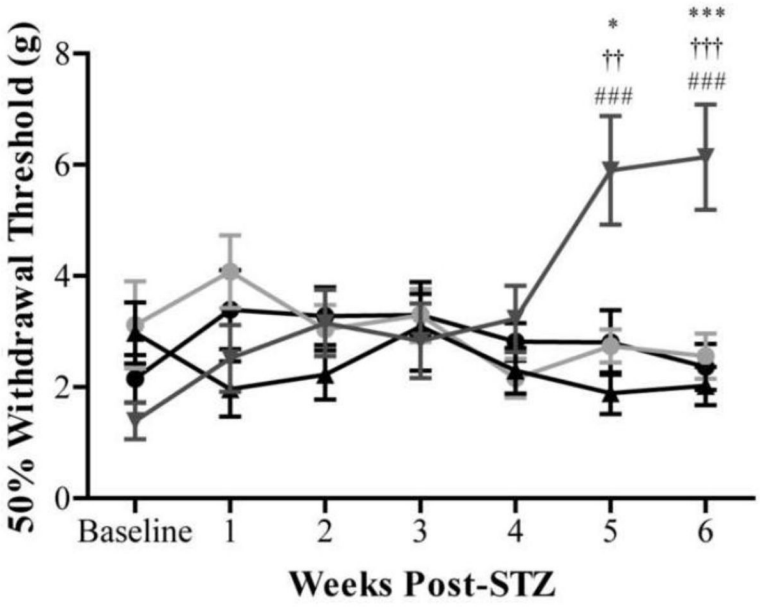

Figure 2. Diabetic BALB/cByJ mice are protected from symptoms of neuropathy, while diabetic BALB/cJ mice develop symptoms insensate neuropathy

Behavioral responses to non-noxious mechanical stimuli were evaluated weekly in nondiabetic BALB/cByJ (black circles), diabetic BALB/cByJ (gray circles), nondiabetic BALB/cJ (black triangles), and diabetic BALB/cJ (gray triangles) mice. Baseline behavioral measurements were similar for all groups tested. By 5 weeks after STZ induction, diabetic BALB/cJ (red $n = 15$) mice developed increased mechanical thresholds indicative of insensate neuropathy. The mechanical thresholds of diabetic BALB/cByJ ($n = 15$) were not different from the thresholds of both nondiabetic strains ($n = 10$ each) at all time points suggesting diabetic BALB/cByJ are protected from neuropathy damage. Data plotted as means ± SEM. *$p < 0.05$ vs. nondiabetic BALB/cByJ. ***$p < 0.001$ vs. nondiabetic BALB/cByJ. ###$p < 0.001$ vs. diabetic BALB/cJ. ††$p < 0.01$ vs. diabetic BALB/cByJ. †††$p < 0.001$ vs. diabetic BALB/cByJ.

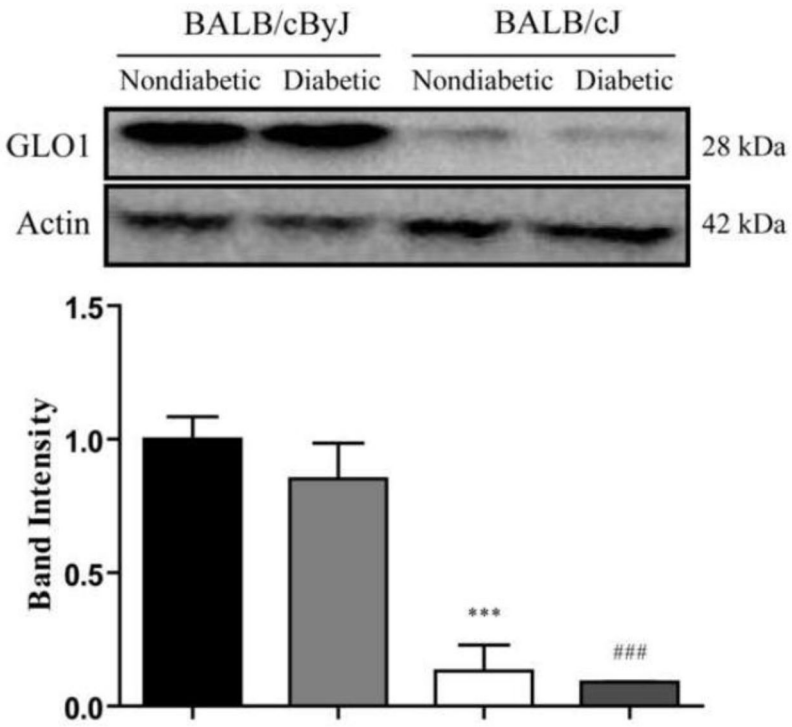

Figure 3. BALB/cByJ mice express higher levels of GLO1 compared to BALB/cJ mice

GLO1 expression in the DRG was measured by Western blot in nondiabetic (n = 3 each) and diabetic mice (n = 4 each) following 6 weeks of diabetes. Nondiabetic BALB/cByJ mice (black bar) express significantly higher levels of GLO1 compared to nondiabetic BALB/cJ mice (white bar). Similarly, diabetic BALB/cByJ mice (light gray bar) also have significantly higher expression of GLO1 compared to diabetic BALB/cJ mice (dark gray bar). Diabetes does not affect the expression of GLO1 in either strain. Diabetic BALB/cByJ and BALB/cJ mice show similar expression levels as their nondiabetic counterparts. Data plotted as means ± SEM. ***$p < 0.001$ vs. nondiabetic Balb/cByJ. ###$p < 0.001$ vs. diabetic Balb/cByJ.

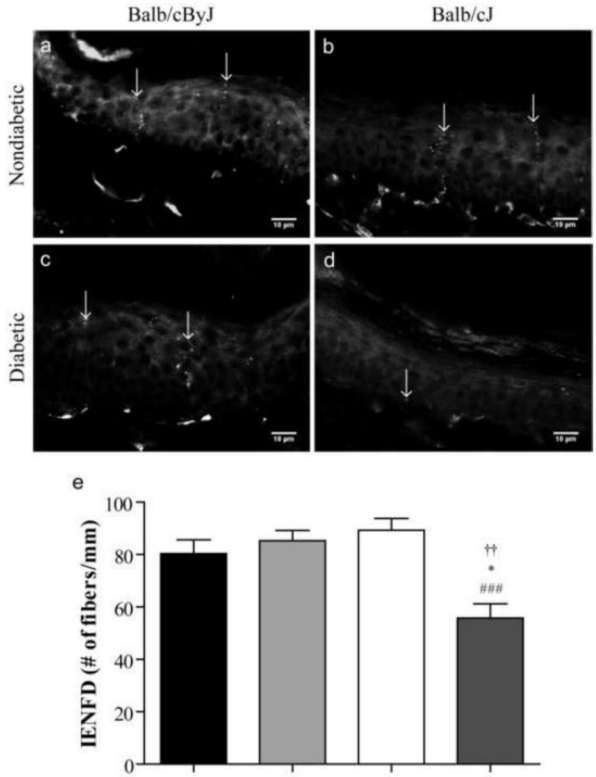

Figure 4. Intraepidermal nerve fiber density is reduced in diabetic Balb/cJ mice

Representative photomicrographs of skin from the right footpad of (a) nondiabetic BALB/cByJ, (b) nondiabetic BALB/cJ, (c) diabetic BALB/cByJ, and (d) diabetic BALB/cJ mice. Diabetic BALB/cJ mice show a reduction in PGP9.5-positive cutaneous nerve fibers in the skin. Scale bar = 10 μm. (e) Quantification of IENFD of nondiabetic BALB/cByJ (black bar, $n = 5$), diabetic BALB/cByJ (light gray bar, $n = 5$), and nondiabetic BALB/cJ (white bar, $n = 5$). Diabetic BALB/cJ (dark gray bar, $n = 5$) have a significant loss of cutaneous innervation after six weeks of diabetes. Data plotted as means ± SEM. ###$p < 0.001$ vs. nondiabetic BALB/cJ. *$p < 0.05$ vs. nondiabetic BALB/cByJ. ††$p < 0.01$ vs. diabetic BALB/cJ.

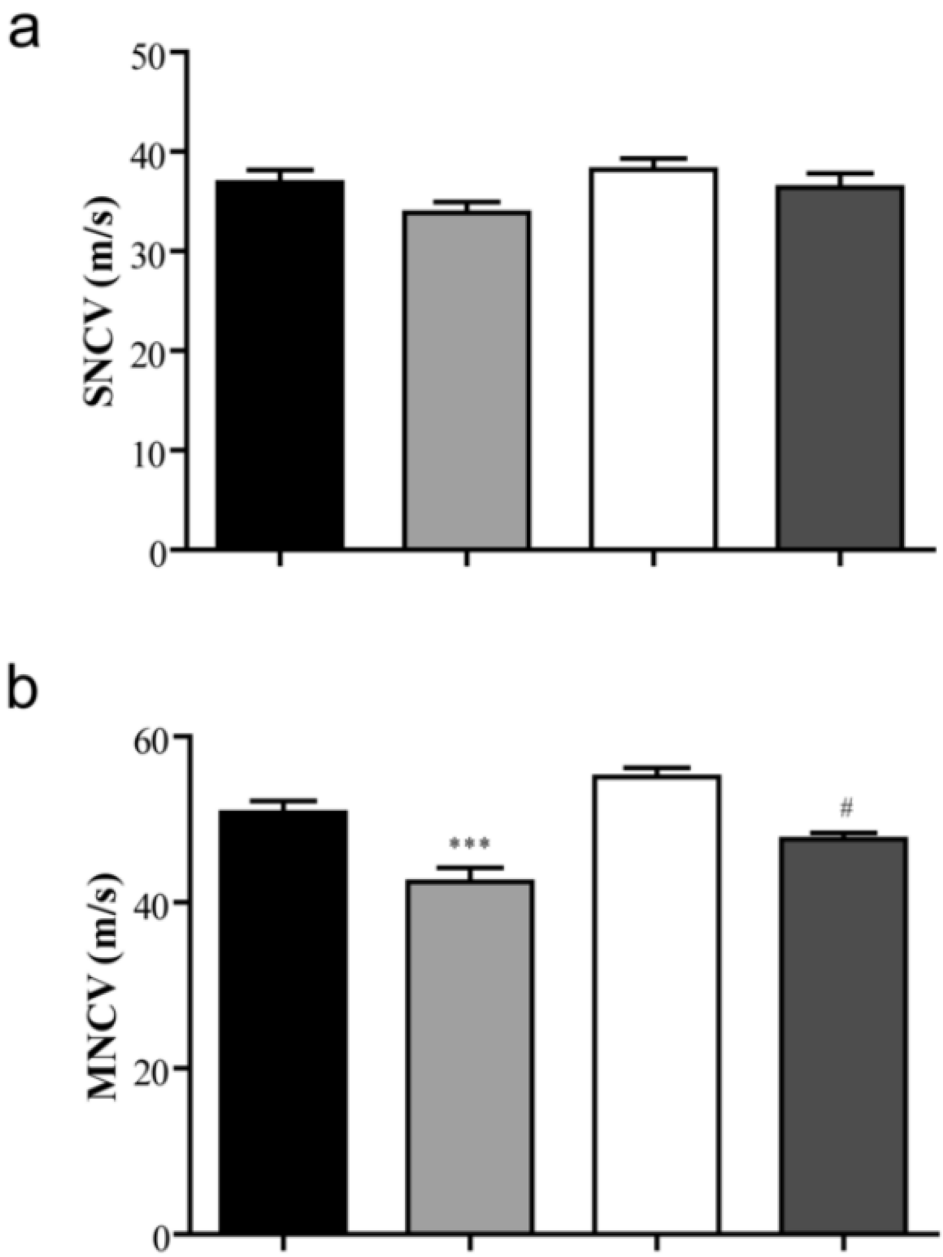

Figure 5. Motor nerve conduction velocity (MNCV), but not sensory nerve conduction velocity (SNCV), is reduced in diabetic mice

Quantification of (a) SNCV and (b) MNCV in nondiabetic BALB/cByJ (black bars, $n = 10$), diabetic BALB/cByJ (light gray bars, $n = 14$), nondiabetic BALB/cJ (white bars, $n = 10$), and diabetic BALB/cJ (dark gray bars, $n = 7$). SNCV is not significantly different between groups. However, MNCV is reduced in diabetic mice compared to their nondiabetic counterparts. Data plotted as means ± SEM. ***$p < 0.001$ vs. nondiabetic BALB/cByJ. #$p < 0.05$ vs. nondiabetic BALB/cJ.

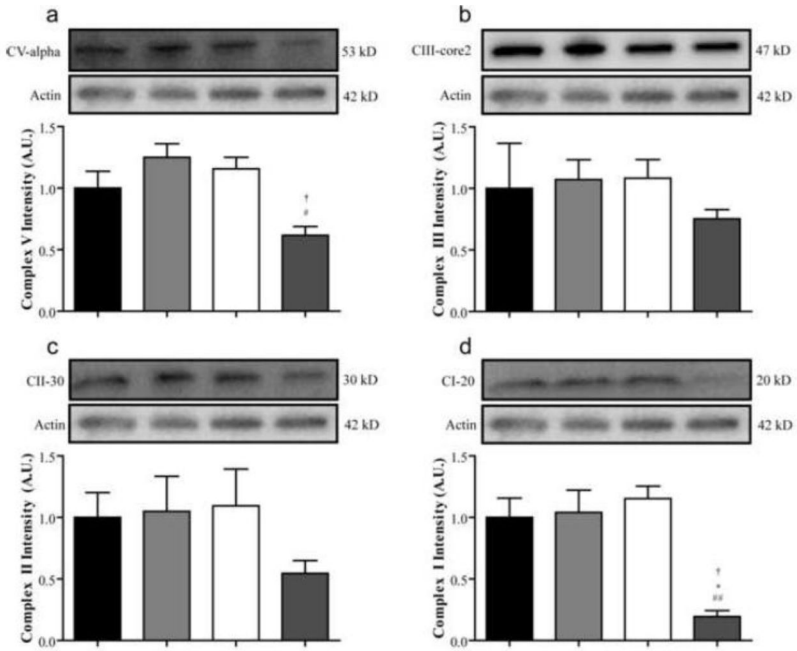

Figure 6. Mitochondrial oxidative phosphorylation proteins are reduced in diabetic BALB/cJ mice

The expression of proteins from mitochondrial oxidative phosphorylation complexes was measured in the DRG after six weeks of diabetes. The expression of structural components of complexes V (a), III (b), II (c), and I (a) were all accessed by Western blot in nondiabetic BALB/cByJ (black bars, $n = 3$), diabetic BALB/cByJ (light gray bars, $n = 3$), nondiabetic BALB/cJ (white bars, $n = 3$), and diabetic BALB/cJ (dark gray bars, $n = 3$). Expression of both ATP synthase subunit α and Complex I subunit NDUFB8 were significantly reduced in diabetic BALB/cJ mice unlike diabetic BALB/cByJ mice. #$p < 0.05$ vs. nondiabetic BALB/cJ. ##$p < 0.01$ vs. nondiabetic BALB/cJ. *$p < 0.05$ vs. nondiabetic BALB/cByJ. †$p < 0.05$ vs. diabetic BALB/cJ.